

SAR change detection based on generalized Gamma distribution divergence and auto-threshold segmentation

GAO Congshan^{1,2}, ZHANG Hong¹, WANG Chao¹, WU Fan¹

1. Center for Earth Observation and Digital Earth, Chinese Academy of Sciences, Beijing 100086, China;

2. Graduate University of Chinese Academy of Sciences, Beijing 100049, China

Abstract: Based on the clutter statistical characteristics of SAR image, this paper takes advantage of the generalized Gamma model to fit the filtered and co-registered SAR images, in order to gain the characteristics information, such as radiation value, local texture, etc. Then, the degree of evolution between the statistical characteristics of multi temporal SAR image is measured by the definition of Kullback–Leibler Divergence in information theory. Afterwards, a combination of KS and KL test has been applied into the evaluation of fitting function for the difference map captured in the former step, which help select the best fitting function automatically for the model-based KI threshold segmentation. Experiment was carried on the multi temporal SAR images for Southern Part of Tianjin, acquired by Radarsat-1/2, as well as Shunyi District of Beijing, acquired by Envisat-ASAR. Such results confirmed the method proposed in this paper not only avoid large number of false alarms generated from the changes of surface corrugation, but also effectively detected the regions ignored by traditional methods, which have no variance in mean value, but differ in texture.

Key words: generalized Gamma, Kullback–Leibler Divergence, KI, SAR, change detection

CLC number: TP722.6 **Document code:** A

Citation format: Gao C S, Zhang H, Wang C and Wu F. 2010. SAR change detection based on generalized Gamma distribution divergence and auto-threshold segmentation. *Journal of Remote Sensing*. 14(4): 710–724

1 INTRODUCTION

With the continuous development of technology and resolution on SAR, space-borne SAR images have been expansively applied into the field of change detection. However, the specificity of SAR imaging mechanism, and the complexity of data processing, brings a number of difficulties to research. In particular, factors like inherent speckle noise, and varying side-looking angle during data acquisition, seriously affect the detection results. Since 1990's, Chinese and international scholars, carried out a series of studies (Fig. 1). Among them, the steps for difference map extraction and threshold segmentation is the hot issue.

In the terms of difference map extraction, owing to the impact of multiplicative speckle noise in SAR image, Rignot (1993) proved theoretically that ratio method would be much more applicable than difference method; moreover logarithmic transformation could effectively compress the scope of the ratio

image. Therefore, the mean ratio detector (MRD) has become the most popular difference map extraction method on multi-temporal SAR image due to its strong advantages, like simplicity and efficiency. Since then, Carvalho (2001) proposed a method of difference map extraction based on wavelet transform; Inglada (2003) introduced the concept of cross entropy (KL) in Information Theory, which calculate the distance between the statistical histogram of image and its fitting probability density function (PDF), into the quantitative measurement of PDFs' difference on multi-temporal SAR image; Mercier (2007) optimized the calculation of KL distance through the application of edgeworth approximation. So far, only some universal classic model, such as Gaussian, Pearson, and Rayleigh distribution, has been applied into the actual work. Considering the complexity and irregularity of the ground objects, a certain bias by the fitting model undoubtedly exist, hence, the selection of clutter model has become a hot issue in the field.

In the terms of threshold segmentation, the traditional method for image process might be divided into three categories: Maximum Classes Square Error Algorithm (Ostu, 1978), Maximum Entropy Algorithm (Shannon, 1979), and Minimum Error Algorithm (Kittler & Illingworth, 1986). Maximum

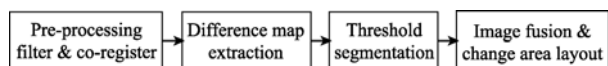


Fig. 1 Main steps for SAR change detection

Received: 2009-05-25; **Accepted:** 2009-08-24

Foundation: National "863" High Technology Research and Development Program of China (No.2009AA12z102) and National Natural Science Foundation of China (No. 40601058, No. 40701108 and No. 40871191).

First author biography: GAO Congshan (1985—), female, master student. She is currently studying at the Center for Earth Observation and Digital Earth, Chinese Academy of Sciences, and specializing in the research for clutter modeling and change detection on SAR image. E-mail: serein_mars@163.com

Classes Square Error Algorithm should be the most efficient method, yet it does not work when the ratio of the size of change and unchanged area in the image is very small (Ulaby, 1986). Although maximum entropy method (THC) can avoid the problem of small proportion between change and unchanged area like OSTU, through the delineation of the scope for threshold selection, it is over-dependent on prior knowledge, which makes the results varying significantly with the choice of different entropy criteria, accordingly the universality of this method is still limited; Minimum error method (KI) is an extension of Bayes minimum error probability theory, its cost function and criterion function varies with the fitting model chosen. Moser (2006) put forward an improved KI Algorithm, which was based on generalized Gaussian Model, and has been widely accepted, in the field of change detection.

Therefore, how to select the best model to describe the clutter statistical characteristics of SAR images, as well as how to extract the best plan to achieve threshold segmentation for difference map, has become the core of change detection research. In this paper, we combined the generalized Gamma distribution to KL divergence in information theory, which effectively quantified the differences between statistical characteristics of multi-temporal SAR image. Then we use a combination of KS and KL Test to select the best fitting model for difference map automatically, thus improving the traditional methods of threshold segmentation KI. The experiment carried out on multi temporal SAR images for Southern Part of Tianjin, acquired by Radarsat-1 and Radarsat-2, as well as Shunyi District of Beijing, acquired by Envisat-ASAR, shows that the KL distance extraction method based on generalized Gamma model could quantify the value of surface radiation characteristics of local changes in texture more accurately, plus the improved KI Threshold Segmentation, the experimental results achieve much better than those of traditional change detection methods.

2 PROBLEM FORMULATION

This paper presents a novel method for SAR change detection, based on generalized Gamma distribution divergence and automatic KI threshold segmentation. Detailed process is shown in Fig. 2. First, we use generalized Gamma model to fit the statistical characteristics of filtered and co-registered SAR images, in order to obtain the characteristics like radiation value and regional texture. Then, apply the definition of KL divergence in information theory to quantify the difference between the statistical characteristics of SAR images. After the extraction of difference map, utilize a combination of KS and KL Test to select the best fitting distribution function for the difference map automatically, so as to achieve KI threshold segmentation based on such model. Among them, the KL difference map extraction based on generalized Gamma and automatic KI threshold segmentation is the core of proposed method.

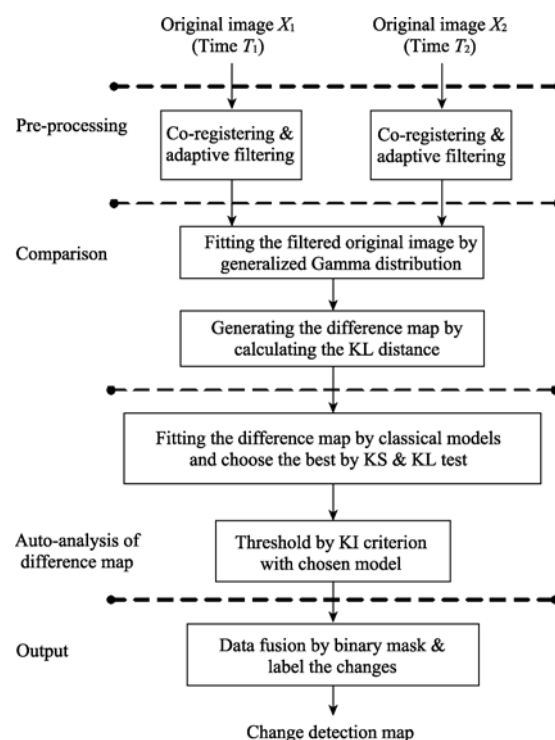


Fig. 2 Flow chart of proposed algorithm

2.1 Generalized Gamma clutter statistical model

The impact of multiplicative speckle noise makes the result of traditional difference and ratio method unsatisfactory. We proposed a method to weaken such impact by calculating the statistical distribution of SAR data in certain area, and then computing the difference between the two distribution functions to reflect the degree of evolution.

According to modeling process, statistical modeling technique was roughly classified into non-parametric and parametric mode. Although non-parametric model seems to be more flexible and suitable for the estimation of unknown complex probability density function, the computation complexity and time consuming caused by its large requirement of sample data, would bring amount of drawbacks (Kittler & Illingworth, 1986), due to its data-driven strategy. In practical, the parametric model is more applicable, the majority of existing, widely used statistical distribution model is evolved from Multiplicative Model (Fig. 3), because of the multiplicative noise characteristics of SAR image.

As the statistical distribution of speckle noise component is determinate, only the statistical distribution of undulated RCS, which express the characterization of the ground objects, need to be taken into account, while doing the statistical modeling of SAR images. In this paper, the 3-parameter generalized Gamma distribution (Eq. (1)) has been chosen as the statistical distribution, of which, $a > 0$, is the shape parameter; $b > 0$ is the scale parameter; c is the power parameters of probability density

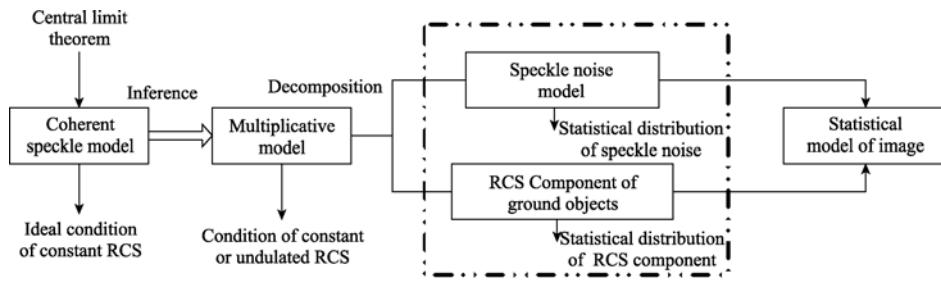


Fig. 3 Statistical distribution model of SAR image developed by product model

distribution. Meanwhile, the shape parameter a and energy parameter c determines the characteristics of clutter distribution.

$$f_{GR-pdf}(x; a, b, c) = \frac{c}{b\Gamma(a)} \left(\frac{x}{b}\right)^{ac-1} \exp\left[-\left(\frac{x}{b}\right)^c\right] \quad (1)$$

The advantages of generalized Gamma distribution, display not only at its more accurate description of heavy-tailed distribution than Rayleigh and Gamma, but also at its characteristic to fit a number of distributions similarly with different estimated parameters. To prove that generalized Gamma could fit different distribution for each sub-region in one image, we show the Fig. 4, which consists of several special modes of generalized Gamma distribution. Thus illustrating that generalized Gamma distribution could be extremely similar to classical models with different estimated parameters, such as Exponential Model ($a=1; c=1$), Rayleigh Model ($a=1; c=2$), Lognormal Model ($a \rightarrow 0$), Weibull Model ($a=1$), Gamma Model ($c=1$), and so on.

$$E[x^k] = \int_0^\infty x^k f_{GR}(x; a, b, c) dx = \int_0^\infty \frac{c}{b\Gamma(a)} \left(\frac{x}{b}\right)^{ac-1} \exp\left[-\left(\frac{x}{b}\right)^c\right] dx = b^k \frac{\Gamma(k/c + a)}{\Gamma(a)} \quad (2)$$

Maximum likelihood (ML) is the most optimal estimation with no prior knowledge. Refer to the recent Chinese and international research, neither the Gradient Ascent Algorithm, nor

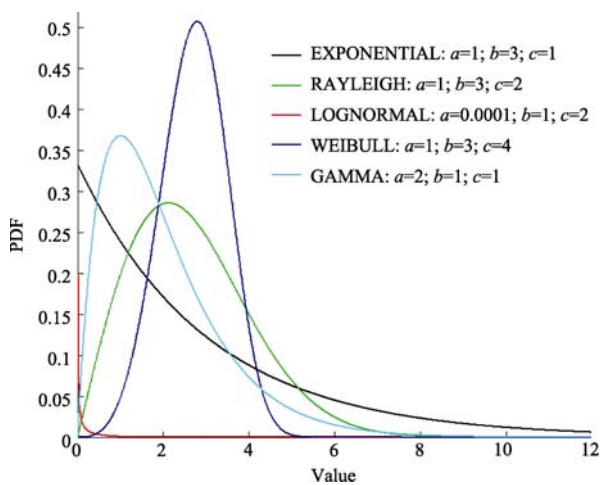


Fig. 4 Classical distribution fitted by generalized Gamma

the Pearson- χ^2 Asymptotic Distance Algorithm (Sharifi & Leon-Garcia, 1995), earns enormous computation consumptions. Therefore, moment estimation has been widely applied into the fitting of large images. The proposed method in this paper, based on the improved parameter estimation method of Generalized Gamma distribution noticed by Gomes (2008), obtains the estimated value of parameters a, b, c through the use of the k -order moment function in Eq.(2).

2.2 Difference map extraction based on KL distance

Use generalized Gamma clutter model mentioned above, to fit for the neighborhood of each pixel, and then utilize Kullback-Leibler divergence (Eq. (3)), referred to cross-entropy, to measure the degree of similarity between two subsets. In other words, that is to reflect the evolution degree of the regional statistics in two-phase image (Jiao, 2008).

$$K(Y|X) = \int \log \frac{f_X(x)}{f_Y(x)} f_X(x) dx \quad (3)$$

where, $f_X(x)$ and $f_Y(x)$ were the generalized Gamma model for the corresponding pixel neighborhood of the T_1 and T_2 two-phase SAR image with the estimated parameters by moment. In order to address the asymmetry in cross-entropy, we used Symmetrised Divergence (Eq. (4)) proposed by Johnson-Sinanovic (2001) or the Jensen-Shannon Divergence (Eq. (5)) proposed by Jeffrey (2000).

$$KLDIV = (K(X|Y) + K(Y|X))/2 \quad (4)$$

$$f_Q(x) = (f_X(x) + f_Y(x))/2 \quad (5)$$

$$KLDIV = (K(Y|Q) + K(X|Q))/2$$

2.3 Auto-KI threshold segmentation

After the extraction of difference map, we need to extract a binary mask to achieve an accurate image orientation of the change region. The classical algorithm is achieved through the identification of threshold for changes. An adaptive threshold segmentation of KI algorithm was proposed in this paper. KI Eq. (7) evolved from Bayes minimum error probability criterion (Eq. (6)). Use criterion function $J(\tau)$ to replace the error probability function $p_{err}(\tau)$; use probability density histogram $h(z)$ to replace the priori probability $P(\omega)$; while the probability of log-likelihood $p(z|\omega, \tau)$ is expressed by the cost function $c(z, \tau)$ (Eq.(8)).

$$p_{\text{err}}(z) = \sum_{\tau=0}^{Z-1} P(\omega_j) p(z | \omega_j, \tau), \quad j=0,1 \quad (6)$$

$$J(\tau) = \sum_{z=0}^{Z-1} h(z) c(z, \tau) \quad (7)$$

$$c(z, \tau) = \begin{cases} -2 \ln p(\omega_0 | z, \tau), & z=1,2,\dots,\tau \\ -2 \ln p(\omega_1 | z, \tau), & z=\tau+1,\tau+2,\dots,Z-1 \end{cases} \quad (8)$$

Based on the Bayesian theory, the posteriori probability of change ω_1 and unchanged ω_0 classes could be calculated by the corresponding prior probability and likelihood probability, the simplified-style is Eq. (9). Therefore, the problem of optimal threshold selection is transformed to obtaining the minimum value of criterion function $J(\tau)$, and then, get the corresponding τ .

$$\hat{P}_{i\tau} = \sum_{z \in R_{i\tau}} h(z)$$

$$c(z, \tau) = \begin{cases} -\ln \hat{P}_{0\tau} - \ln p_0(z | \hat{m}_{0\tau}, \hat{\sigma}_{0\tau}), & z < \tau + 1; \\ -\ln \hat{P}_{1\tau} - \ln p_1(z | \hat{m}_{1\tau}, \hat{\sigma}_{1\tau}), & \tau < z < Z \end{cases} \quad (9)$$

$$J(\tau) = \sum_{z=0}^{Z-1} h(z) c(z, \tau)$$

$$T = \arg \min \{ J(\tau) : \tau=0,1,2,\dots,Z-1 \}$$

Since KL difference map captured from different origin image or different cluster fitting model, may be in line with the different distribution. Accordingly, generalized Gauss, G_0 , and the Joint Lognormal & Rayleigh distribution model had been introduced to fit the obtained difference map in this paper. Moreover, a combination of KS and KL test has been applied to select the best fitting function automatically, and then, the model-based threshold segmentation KI could be operated.

3 EXPERIMENTAL RESULTS

3.1 Experimental dataset

In this paper, the multi-temporal SAR images for Southern Part of Tianjin (Fig. 5), and Shunyi District of Beijing (Fig. 6) has been used, the detail is shown in Table 1.

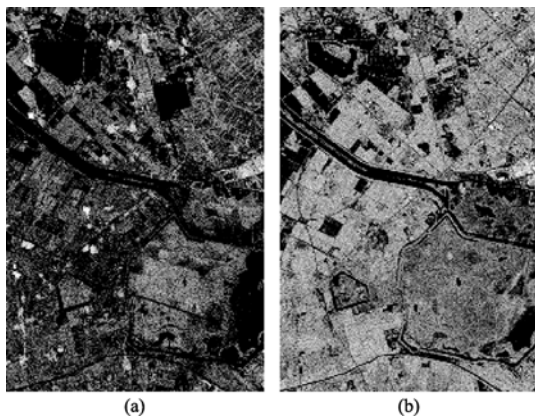


Fig. 5 Southern Part of Tianjin
(a) Radarsat-1 2001-11-14; (b) Radarsat-2 2008-10-22

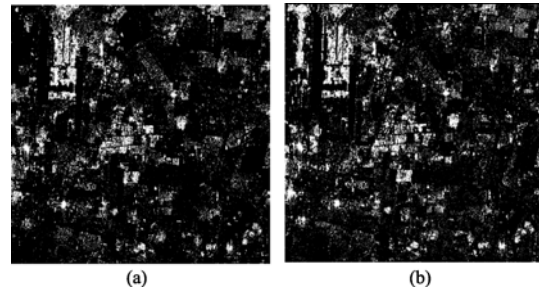


Fig. 6 International Airport in Beijing
(a) ASAR 2004-06-01; (b) ASAR 2005-05-17

Table 1 Experiment dataset*

| Area | Tianjin | Tianjin | Beijing Shunyi | Beijing Shunyi |
|----------------------------|-------------|-------------|----------------|----------------|
| Time | 2001-11-14 | 2008-10-22 | 2004-06-01 | 2005-05-17 |
| Sensor | RADAR SAT-1 | RADAR SAT-2 | ASAR | ASAR |
| Polarization | HH | HH | HH | HH |
| Resolution /m ² | 10×8 | 10×8 | 30×30 | 30×30 |
| Image size /pixel | 1770×2650 | 1770×2650 | 1024×1024 | 1024×1024 |

*All neighborhood window size selected as 7×7

3.2 Comparison between different methods for difference map extraction

Mean-Ratio Detector (MRD) is the most commonly used difference map extraction method on multi-temporal SAR Image. However, Ulaby (1986) pointed out that classical distribution of SAR image texture is mostly based on the zero-mean multiplicative model assumption. Therefore, in SAR image, when the windows get large, the phenomenon that mean value of the window remains the same while the texture changes, would be ignored by the MRD detector (Fig. 7). Similarly, when the window is too small, the texture does not change, while the overall window brightens or darkens because of noise or changes in external conditions, and therefore the MRD detector may cause false alarms.

Therefore, the proposed method makes use of the characteristics of generalized Gamma distribution, which could be similar to different distribution with various parameter estimation, to describe the statistical characteristics of clutter in SAR image. Then the definition of KL divergence is used, which was put forward in information theory to calculate difference between fitting PDF and statistical histogram, so as to characterize the evolution of two SAR images, and generate the difference map.

As shown in Fig. 7, MRD method was applied to the two images of Tianjin Province captured by Radarsat-1/2 on January 14th 2001 and October 22nd 2008. However, the result shows a large amount of false alarm in the field of water. On the contrast, the proposed method in this paper solved this problem effectively through the use of KL distance with generalized Gamma distribution at the step of obtaining difference map, as shown in Fig. 8.

In order to further verify the superiority of the extraction method based on KL difference map with generalized Gamma



Fig. 7 MRD



Fig. 8 G-Gamma

distribution, this paper selected three corresponding sample area (Fig. 9) from Fig. 5 for experiments. A is the Yadian Reservoir of Xiqing District; B is the Jinnan Reservoir; C is the

Beidagang Wetland Nature Reserve. The total size of the known sample area is 1186048 pixels, of which the number of actual change pixel is 174608, unchanged pixel is 1011440 pixels. Take the statistics for detection rate and false alarm rate of both the proposed and MRD method based on different thresholds, and then draw ROC (Receiver Operating Characteristics).



Fig. 9 Sample area

ROC analysis originated in statistical decision theory, and has been applied to observe the ability of radar signal evaluation since 1950's. The primitive application is to judge the receivers' ability to extract useful information from the signal and noise mixed-waveforms. Since 2003, scholars like Inglada, has expanded its application to the performance evaluation of difference map extraction methods on SAR image change detection, thus could reflect the relationship between detection rate (vertical axis) and false alarm rate (horizontal axis) for each detector. The main application is: consider the image as a binary array with two values, that is change and unchange, for all possible thresholds, calculate the portfolio between detection rate (P_{det}) and false alarm rate (P_{fa}) for each operator. Then draw and line them in the coordinate. When the threshold value reached the up-limit, all pixels would be regarded as unchanged, resulting in P_{det} and P_{fa} both equal to 0, which is also the operating point at lower-left corner of ROC. Meanwhile, P_{det} and P_{fa} would correspondingly increase with the decrease for threshold selected. While the threshold value reached the down-limit, all pixels would be regarded as change, resulting in P_{det} and P_{fa} both equal to 1, thus is consistent to the operating point at the upper right corner of ROC curve.

For ROC the greater the area below curve is, the better effect the detection method would be (Huo, 2008). Therefore, as showed in Fig. 10, the effect of the proposed KL detector based on generalized Gamma (Red) is significantly superior to the traditional MRD (Blue) difference map extraction method. Moreover, the KL detector based on Rayleigh (Green) is just located between the two.

3.3 Selection of fitting function for difference map

This paper selected three different kinds of KL difference maps to convince the complexity and uncertainty of their distribution, containing one for Beijing by generalized Gamma, one for Tianjin by generalized Gamma, and one for Tianjin by Rayleigh. Then, utilize a combination of KS and KL Test to evaluate PDFs for different model, in order to select the best fitting one for the difference map automatically.

KS test is a non-parametric estimation, used to test whether the distribution fit the known theoretical distribution or not. It has been widely applied into various fields of statistical model fitting test by many scholars since 1967. While KS test requires cumulative distribution function (CDF) of fitting model, both approaches for computing CDF of generalized Gauss, which are constructing the upper bound function and the stochastic differential equation, would have an impact on the simulation results with the selection of corresponding random number or the coefficient for reaction-diffusion equation. Therefore, this paper realize the selection of the best fitting model, by calling the KL test proposed in section 2.2, to evaluate and compare the best fitting model selected through KS test, as well as the model of generalized Gauss.

From Table 2 and Table 3, for the KL difference map of Beijing based on Generalized Gamma Distribution, the Rayleigh & Lognormal joint distribution fits best; for the KL difference map of Tianjin based on Generalized Gamma Distribution, the

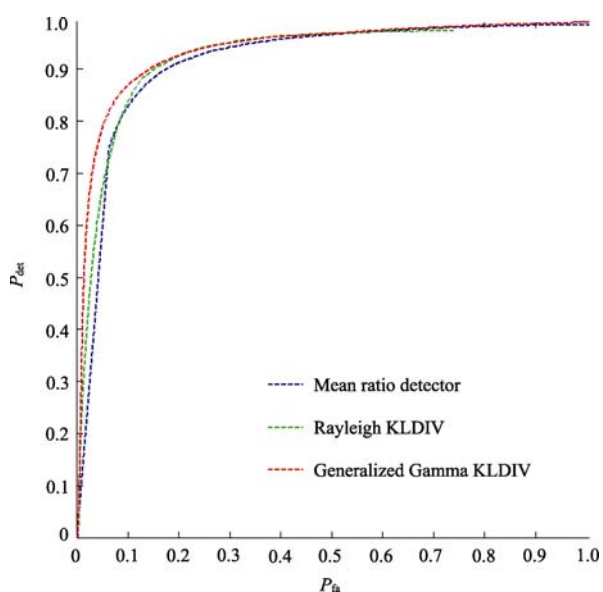


Fig. 10 ROC curve for different detectors

Table 2 KS test results for different fitting model

| Kolmogorov-Smirnov (KS) | Beijing GGamma KLDIV | Tianjin GGamma KLDIV | Tianjin Rayleigh KLDIV |
|-------------------------|----------------------|----------------------|------------------------|
| LOGNORMAL | 0.04593 | 0.059662 | 0.075721 |
| GAMMA | 0.10155 | 0.030702 | 0.086152 |
| RAYLEIGH | 0.47975 | 0.10716 | 0.46306 |
| WEIBULL | 0.08565 | 0.050324 | 0.08876 |
| K | 0.14910 | 0.041051 | 0.10292 |
| MIX (RAY&LN) | 0.02193 | 0.027327 | 0.064636 |
| G0 | 0.07289 | 0.026651 | 0.38563 |

Table 3 KL test results for best fitting model and generalized Gauss model

| Jensen-Shannon (KL) | Beijing GGamma KLDIV | Tianjin GGamma KLDIV | Tianjin Rayleigh KLDIV |
|---------------------|----------------------|----------------------|------------------------|
| G0 | 0.0828 | 0.0473 | 0.1630 |
| G-Gauss | 0.1900 | 0.2086 | 0.1704 |
| MIX (RAY&LN) | 0.0473 | 0.0561 | 0.0271 |

G0 distribution fits best; for the KL difference map of Beijing based on Rayleigh Distribution, also the Rayleigh & Lognormal joint distribution fits best. That is to say, although the generalized Gauss model fits MRD difference map very well, it does not work towards the proposed method in this paper. Such confirms that if both the selection of different features or different distribution model for SAR image fitting may influence the distribution of KL difference map generated. Therefore, the method used in this paper is necessary and feasible.

3.4 Threshold segmentation and result evaluation

Still use the two images for Southern Part of Tianjin, acquired by Radarsat-1/2, as an example (Fig. 5). First, extract KL difference map based on generalized Gamma (Fig. 8), and then call the KS test (Fig. 11) to assess all the fitting distribution models. According to the second column in Table 2, it shows G0 model, which is applicable to uneven region, fits the best, so operating the KI threshold segmentation by G0 (Fig. 12).

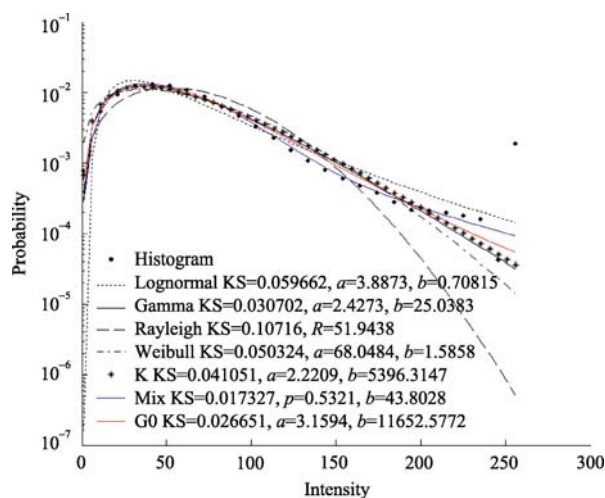


Fig. 11 KS test for G-Gamma KL difference map



Fig. 12 Auto-KI segmentation for G-Gamma KLDIV

In the academic field of SAR image change detection, many scholars, led by Lorenzo Bruzzone, focused their study on the optimization and expansion for KI threshold segmentation with MRD differences map, based on generalized Gauss, and won great progress. Therefore, this paper also used this method to detect the change area of Tianjin with the image captured in 2001 and 2009. According to the on-site survey, the main changes should be the construction of the Island Project for Yadian Reservoir in April 2007, the cultivation of fruits and aquaculture industry in Jinnan Reservoir in 2003, and the substantially reduced wetlands area in Beidagang at recent years.

In order to compare this method with the one proposed in this paper intuitively, we use edge tracking algorithm to draw the border region information of the binary change mask in the original images (Fig. 13, Fig. 14).

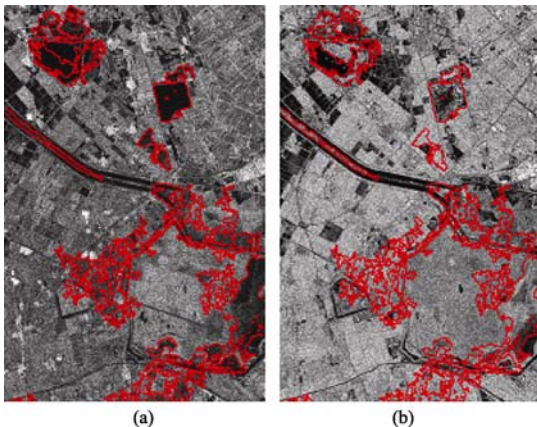


Fig. 13 Southern part of Tianjin
(a) Radarsat-1 2001-11-14; (b) Radarsat-2 2008-10-22

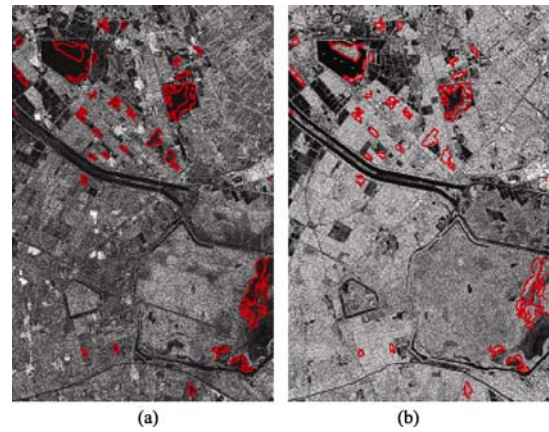


Fig. 14 International airport in Beijing
(a) Radarsat-1 2001-11-14; (b) Radarsat-2 2008-10-22

As seen, the KI threshold segmentation based on generalized Gauss is indeed an effective method to avoid the false alarm caused by corrugated surface in MRD progress. But at the same time, for changes taken place in small regions, it was not sensitive enough. The experimental results show that the method proposed in this paper has effectively solved this problem, and detect the unchanged area in Jinnan Reservoir and Beidagang Wetland, which was missed by generalized Gauss KI Algorithm. In short, the method used in this paper, performance better in the detail description for changes of small region.

4 DISCUSSION AND CONCLUSIONS

This paper presents a novel method for SAR change detection, based on generalized Gamma distribution divergence and adaptive KI threshold segmentation. This method particularly calculates the KL difference map by generalized Gamma model, so as to effectively overcome the problem of information loss in local texture characteristics, happened by traditional MRD method; at the same time, made a combination of KS and KL test, which realized the adaptation KI threshold segmentation. In this paper, experiment was carried out on the multi temporal SAR images for Southern Part of Tianjin, acquired by Radarsat-1/2, and Shunyi District of Beijing, acquired by Envi-sat-ASAR. Such results confirmed that the method proposed in this paper could accurately obtain the radiation value and texture information through an effective statistical characteristics fitting of SAR images. Compared with traditional change detection methods, the proposed approach may bring a more satisfactory effect, especially for those changes in farmland species, wetlands, and some other small region. The further optimization and efficiency of this method, as well as the further integration with image feature extraction algorithm (Gamba, 2006) will be the focus of the study in the next step.

REFERENCES

Carvalho L M T and Fonseca L M G. 2001. Digital change detection with the aid of multiresolution wavelet analysis. *International*

Journal of Remote Sensing, **4**(5): 3871—3876

- Chatelain F and Inglada J. 2008. Change detection in multisensor SAR images using bivariate gamma distributions. *IEEE Transaction on Image Processing*, **17**(3): 249—258
- Gamba P, Dell'Acqua F and Lisini G. 2006. Change detection of multi-temporal SAR data in urban areas combining feature-based and pixel-based techniques. *IEEE Transactions on Geoscience and Remote Sensing*, **144**(10): 2820—2827
- Gomes O, Combes C and Dussauchoy A. 2008. Parameter estimation of the generalized gamma distribution. *Mathematics and Computers in Simulation*, **79**(4): 955—963
- Huo Chun-lei. 2008. Object-level change detection based on multiscale fusion. *Acta Automatica Sinica*, **34**(3): 251—257
- Inglada J. 2003. Change detection on SAR images by using a parametric estimation of the Kullback-Leibler divergence. In Proc. IGARSS Toulouse. France
- Jiao Li-chen. 2008. Intelligent SAR Image Processing and Interpretation. Beijing: Science Press
- Kittler J and Illingworth J. 1986. Minimum error thresholding. *Pattern Recognition*, **19**(1): 41—47
- Kuang Gang-yao. 2007. Synthetic Aperture Radar Target Detection Theory Algorithm and Application. Beijing: University of Defense Technology Press
- Mercier G and Derrode S. 2004. SAR image change detection using distance between distributions of classes. *IEEE Transactions on Geoscience and Remote Sensing*, **74**(4): 3872—3875
- Mercier G and Inglada J. 2007. A new statistical similarity measure for change detection in multitemporal SAR images and its extension to multiscale change analysis. *IEEE Transactions on Geoscience and Remote Sensing*, **45**(5): 1432—1445
- Moser G. 2008. Conditional copulas for change detection in heterogeneous remote sensing images. *IEEE Transactions on Geoscience and Remote Sensing*, **46**(5): 1147—1153
- Moser G. 2007. Unsupervised change detection from multichannel SAR images. *IEEE Letters. Geoscience and Remote Sensing*, **4**(2): 278—282
- Moser G and Serpico S B. 2006. Generalized minimum-Error thresholding for unsupervised change detection from SAR amplitude imagery. *IEEE Transactions on Geoscience and Remote Sensing*, **44**(10): 2972—2982
- Oliver C. 2004. Understanding Synthetic Aperture Radar Images: SciTech Publishing
- Rignot E, Zyl J M and Van J. 1993. Change detection techniques for ERS-1 SAR data. *IEEE Transactions on Geoscience and Remote Sensing*, **31**(4): 896—906
- Sharifi K and Leon-Garcia A. 1995. Estimation of shape parameter for generalized Gaussian distributions in subband decomposition of video. *IEEE Trans. Circuits, Syst. Video Technol*, **1**(5): 52—56
- Uiaby F T and Kouyate F. 1986. Textural information in SAR images. *IEEE Transactions on Geoscience and Remote Sensing*, **24**(2): 235—245

广义 Gamma 模型及自适应 KI 阈值分割的 SAR 图像变化检测

高丛珊^{1,2}, 张红¹, 王超¹, 吴樊¹

1. 中国科学院 对地观测与数字地球科学中心, 北京 100086;

2. 中国科学院 研究生院, 北京 100049

摘要: 基于 SAR 图像的杂波统计特性, 利用广义 Gamma 模型对降噪配准后的 SAR 图像统计特征进行拟合, 获取了辐射值与局部纹理等特征信息; 采用信息论中交叉熵的概念, 量化不同时相 SAR 图像统计特征间的差异程度; 利用 KS 与 KL 检验相结合, 自动选取对差异图拟合情况最好的模型, 从而实现基于该模型的 KI 阈值分割。通过对天津市北辰区以南地区的两幅 Radarsat 图像, 以及北京市顺义区的两幅 ASAR 图像的实验表明, 所提出的方法不仅有效地避免了水面波纹变化所产生的大量虚警, 并能有效地检测出传统方法所不能识别的, 区域内均值不变, 仅纹理发生变化的情况。

关键词: 广义 Gamma, K-L 散度, KI 法则, SAR, 变化检测

中图分类号: TP722.6

文献标识码: A

引用格式: 高丛珊, 张红, 王超, 吴樊. 2010. 广义 Gamma 模型及自适应 KI 阈值分割的 SAR 图像变化检测. 遥感学报, 14(4): 710—724

Gao C S, Zhang H, Wang C and Wu F. 2010. SAR change detection based on generalized Gamma distribution divergence and auto-threshold segmentation. *Journal of Remote Sensing*, 14(4): 710—724

1 引言

随分辨率的不断提高, SAR 图像越来越多地应用到变化检测工作中。但 SAR 成像机理的特殊性和数据处理的复杂性, 给变化检测带来了诸多困难。尤其是其固有的斑噪、数据获取侧视角度等因素, 严重影响了检测结果。因此, 该领域自 20 世纪 90 年代起, 针对 SAR 图像变化检测主要 4 个环节(图 1), 开展了一系列的研究。其中, 以差异图提取与阈值分割的环节最为核心。

差异图提取方面, 考虑到乘性斑噪的影响, Rignot(1993)指出比值法较差值法更适用, 且对数变换能有效压缩比值图像的变化范围, 均值对数比(MRD)

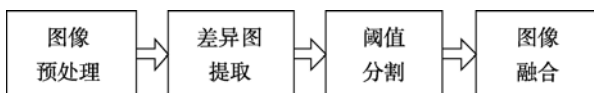


图 1 SAR 图像变化检测主要流程

因其简单高效的特点, 得到了广泛应用。但其对区域内均值不变、纹理改变的情况不够敏感, Carvalho(2001)提出了基于小波变换的差异图提取法; Inglada(2003)引入了信息论中交叉熵(KL)的概念, 以计算多时相 SAR 图像概率密度函数(PDF)间的距离; Mercier(2007)用边沿级数逼近对 KL 计算进行了优化。目前, 仅高斯、皮尔森、瑞利等模型被应用到差异图提取工作中, 而实际的地面情况往往十分复杂, 简单的模型已不能满足需求, 其优化问题成为了该领域的热点。

阈值分割方面, 传统方法主要分为: 最大类间方差法(OSTU)、最大熵法(THC)、最小误差法(KI)等。其中, 以 OSTU 法效率最高, 但实验证明该方法在图像目标与背景的面积比很小时失效(Kittler & Illingworth, 1986), 变化检测方面, 变化区域的面积往往有限, 该方法不适用; THC 法虽可通过圈定阈值选取范围, 避免 OSTU 中目标与背景比例过小的

收稿日期: 2009-05-25; 修订日期: 2009-08-24

基金项目: 国家 863 项目(编号: 2009AA12z102)、国家自然科学基金(编号: 40601058, 40701108, 40871191)。

第一作者简介: 高丛珊(1985—), 女, 硕士研究生, 现就读于中国科学院对地观测与数字地球科学中心, 目前主要从事 SAR 图像杂波建模与变化检测方面的研究工作。E-mail: serein_mars@163.com。

问题, 但范围的设定过分依赖先验知识, 使结果易随选择的熵准则不同产生很大差异, 故普遍性不广; KI 法则是 Bayes 最小错误概率理论的延伸, 其代价函数与决策函数随所选拟合模型的不同而变化。其中以 Moser(2006)提出的基于广义高斯模型的 KI 法最为著名。

本文将广义 Gamma 分布模型与信息论中 KL 散度的概念结合到一起, 有效地量化了二时相 SAR 图像的统计特征差异; 并采用了一种 KS 与 KL 结合的评价方法, 实现对差异图最优拟合函数的自动选取, 从而改进了传统 KI 阈值分割方法。通过对天津市北辰区以南的 Radarsat-1 和 Radarsat-2 图像, 及北京顺义区的两幅 Envisat-ASAR 图像进行实验, 验证了基于广义 Gamma 模型的 KL 差异图提取方法能较准确地量化地表辐射值与局部纹理等特征的变化程度, 且通过本文改进的 KI 阈值分割步骤可获得较之传统变化检测方法, 更为理想的效果。

2 算法流程

提出了一种基于广义 Gamma 分布模型的 KL 差异图提取及自适应 KI 阈值分割的新方法(图 2)。

2.1 广义 Gamma 杂波统计模型

SAR 图像固有的斑噪, 使传统的差值、比值等方法检测效果不理想。通过求取 SAR 图像一定区域内的统计分布模型, 来削弱其影响; 使用两个分布函数之间的差异来表征两幅图像间的差异。

SAR 图像统计建模技术按其建模过程可粗略分为参量模型和非参量模型(Oliver, 2004)。非参量模型建模灵活, 适合对未知的复杂概率密度函数进行参数估计, 但需大量的样本数据, 从而带来了操作复杂、计算耗时等问题。在实际应用中, 参量模型更为适用。基于 SAR 图像乘性斑噪的特点, 大多数现有的、广泛应用的统计分布模型, 都是由乘积模型发展而来的(图 3)。

由于 SAR 图像斑点噪声分量的统计分布是确定的, 其统计模型只需考虑表征地物真实 RCS 起伏的统计分布即可。本文选用的广义 Gamma 分布(式(1))是一个 3 参数统计分布模型, 其中, a 是形状参数; b 是尺度参数; c 是能量参数。形状参数 a 与能量参数 c 决定了杂波分布的特性。

采用广义 Gamma 分布, 可以比 Rayleigh 和 Gamma 分布更精确地描述拖尾严重的情况, 而且可以利用广义 Gamma 函数随不同的参数估计结果, 近似拟合多种不同分布的特性, 来对同一幅图像中各子区域具有不同特征的情况, 进行拟合。如图 4, 各种标准的杂波模型, 如指数模型($a=1; c=1$)、瑞利模型($a=1; c=2$)、对数正态模型($a \rightarrow 0, \infty$)、韦布模型($a=1$)、伽玛模型($c=1$)等, 都是广义 Gamma 模型的特例。

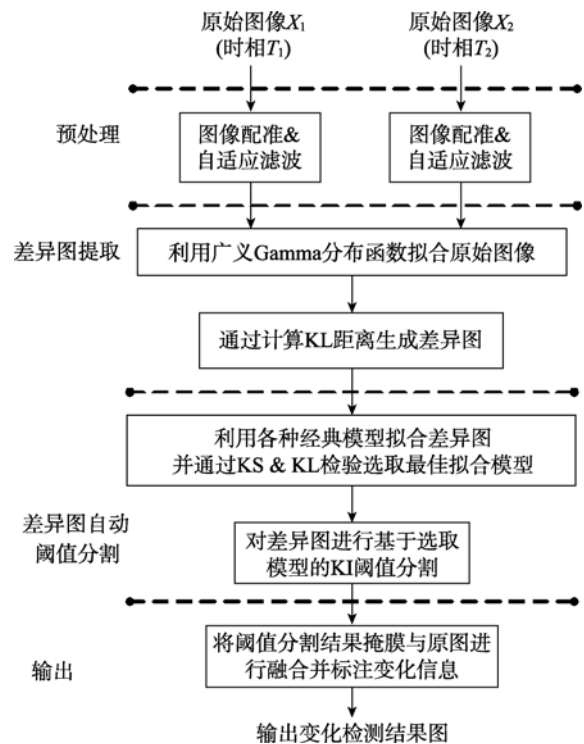


图 2 算法主要流程

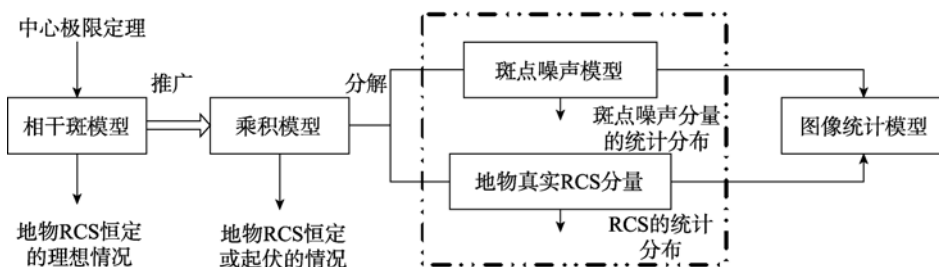


图 3 由乘积模型发展起来的 SAR 图像统计分布模型(匡纲要等, 2007)

$$f_{\Gamma\text{-pdf}}(x; a, b, c) = \frac{c}{b\Gamma(a)} \left(\frac{x}{b}\right)^{ac-1} \exp\left[-\left(\frac{x}{b}\right)^c\right] \quad (1)$$

$$\begin{aligned} E[x^k] &= \int_0^\infty x^k f_{\Gamma}(x; a, b, c) dx \\ &= \int_0^\infty \frac{c}{b\Gamma(a)} \left(\frac{x}{b}\right)^{ac-1} \exp\left[-\left(\frac{x}{b}\right)^c\right] dx \quad (2) \\ &= b^k \frac{\Gamma(k/c + a)}{\Gamma(a)} \end{aligned}$$

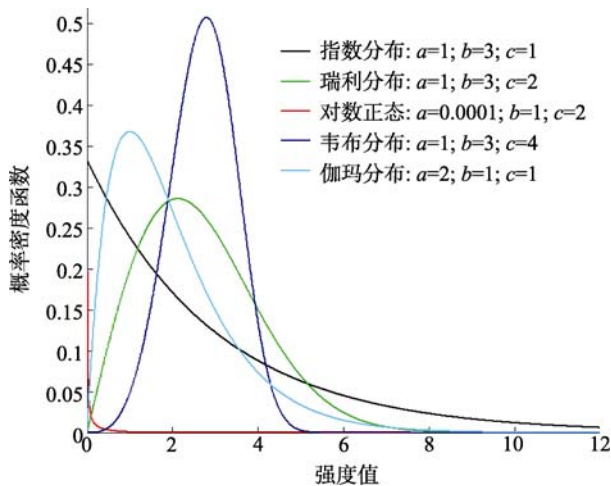


图4 广义 Gamma 拟合的经典分布

最大似然法(ML)是无先验知识情况下的最优估计方法。根据目前的研究现状,无论是利用梯度上升,还是 Pearson- χ^2 距离渐近等算法(Sharifi & Leon-Garcia, 1995),其计算量都过于庞大,所以对大尺寸图像进行拟合时,通常采用矩估计的方法快速有效地获取参数估计值。本文采用 Gomes(2008)提出的改进的广义 Gamma 分布参数估计方法,利用 k 阶矩函数(式(2)),来获取 a, t, c 3 个参数的估计值。

2.2 基于 K-L 距离的差异图提取

选用上述广义 Gamma 杂波模型的概率密度函数对各像元邻域进行拟合,再利用 Kullback-Leibler 散度,即交叉熵,刻画两个子集之间的相似程度(式(3)),即通过判断其统计特性的变化,反映两个时相图像区域统计的变化程度(Mercier & Derrode, 2004)。

$$K(Y|X) = \int \log \frac{f_X(x)}{f_Y(x)} f_X(x) dx \quad (3)$$

式中, $f_X(x)$ 与 $f_Y(x)$ 分别为经矩估计获取参数后,得到的 T_1 与 T_2 两个时相 SAR 图像中对应像元邻域内的广义 Gamma 模型。为了解决交叉熵的不对称性,可以采用 Johnson-Sinanovic(2001)提出的规则化处理方法(式(4))或者 Jensen-Shannon(2000)提出的 Jeffrey 平衡法(式(5))解决。

$$KLDIV = (K(X|Y) + K(Y|X))/2 \quad (4)$$

$$f_Q(x) = (f_X(x) + f_Y(x))/2 \quad (5)$$

$$KLDIV = (K(Y|Q) + K(X|Q))/2$$

2.3 自适应 KI 阈值分割

差异图提取后,为在原图准确定位变化区域,需提取变化与未变化类的二值化掩模,经典算法是通过确定变化阈值实现的。本文提出了一种自适应的 KI 阈值分割方法。KI 法则(式(7))是从 Bayes 最小错误概率准则(式(6))演化而来。用决策函数 $J(\tau)$ 取代错误概率函数 $p_{\text{err}}(z)$; 概率密度直方图 $h(z)$ 则代替先验概率 $P(\omega_j)$; 对数似然概率 $p(z|\omega_j, \tau)$ 由代价函数 $c(z, \tau)$ 表达(式(8))。

$$p_{\text{err}}(z) = \sum_{j=0}^{Z-1} P(\omega_j) p(z|\omega_j, \tau), \quad j=0,1 \quad (6)$$

$$J(\tau) = \sum_{z=0}^{Z-1} h(z) c(z, \tau) \quad (7)$$

$$c(z, \tau) = \begin{cases} -2 \ln p(\omega_0|z, \tau), & z=1,2,\dots,\tau \\ -2 \ln p(\omega_1|z, \tau), & z=\tau+1,\tau+2,\dots,Z-1 \end{cases} \quad (8)$$

其中变化类 ω_1 与未变化类 ω_0 的后验概率可根据贝叶斯理论,用对应的先验概率和似然概率求取,经简化可得式(9)。最佳阈值的选取问题即转化为求取决策函数 $J(\tau)$ 最小值的问题,进而获取对应的 τ 。

$$\begin{aligned} \hat{P}_{\text{tr}} &= \sum_{z \in R_{\text{tr}}} h(z) \\ c(z, \tau) &= \begin{cases} -\ln \hat{P}_{0\tau} - \ln p_0(z|\hat{m}_{0\tau}, \hat{\sigma}_{0\tau}), & z < \tau + 1; \\ -\ln \hat{P}_{1\tau} - \ln p_1(z|\hat{m}_{1\tau}, \hat{\sigma}_{1\tau}), & \tau < z < Z \end{cases} \quad (9) \end{aligned}$$

$$J(\tau) = \sum_{z=0}^{Z-1} h(z) c(z, \tau)$$

$$T = \arg \min \{J(\tau) : \tau=0,1,2,\dots,Z-1\}$$

对不同地物,或使用不同拟合模型获取的 KL 差异图,结果可能近似于不同的分布模型,因此,仅使用经典模型进行拟合,效果不理想。因此,本文引入广义 Gauss、G0, 及 Lognormal 和 Rayleigh 联合分布等模型,同时对差异图进行拟合,并使用 KS 与 KL 检验相结合的方法评估拟合优度,自动选取最优拟合函数,并进行基于该模型的 KI 阈值分割。

3 实验与结果

3.1 实验数据

本文使用天津市北辰区以南(图 5)、北京市顺义区(图 6)两组 SAR 图像,成像信息如表 1。

表 1 实验数据*

| 地区 | 天津市北辰区以南 | 天津市北辰区以南 | 北京市顺义区 | 北京市顺义区 |
|--------------------|-------------|-------------|------------|------------|
| 成像日期 | 2001-11-14 | 2008-10-22 | 2004-06-01 | 2005-05-17 |
| 传感器 | RADAR SAT-1 | RADAR SAT-2 | ASAR | ASAR |
| 极化方式 | HH | HH | HH | HH |
| 分辨率/m ² | 10×8 | 10×8 | 30×30 | 30×30 |
| 图像尺寸(pixel) | 1770×2650 | 1770×2650 | 1024×1024 | 1024×1024 |

* 本文中所有实验选取邻域窗口大小为 7×7

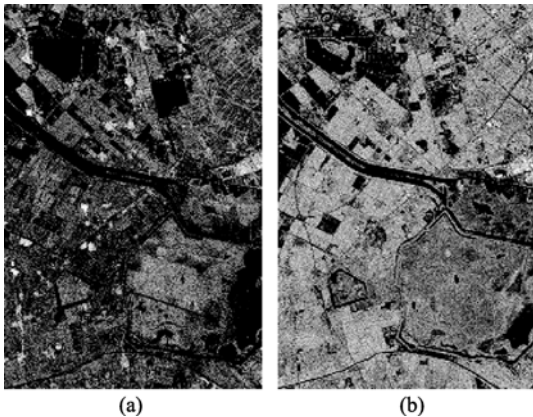


图 5 天津市北辰区以南
(a) 2001-11-14; (b) 2008-10-22

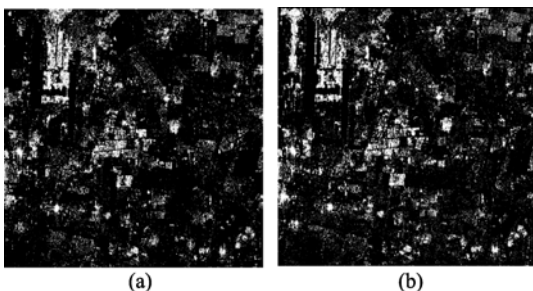


图 6 北京顺义国际机场周边
(a) 2004-06-01; (b) 2005-05-17

3.2 差异图提取方法比较

均值对数比检测器(mean-ratio detector, MRD)是目前最常用的多时相 SAR 图像差异图提取方法。但 Ulaby(1986)曾指出,经典的 SAR 图像纹理分布多数是基于零均值乘性模型的假设。因此,对 SAR 图像,窗口取得较大时,易发生邻域内均值不变,仅纹理发生变化的情况,MRD 方法将无法检测,发生漏检;同样,若窗口过小,对纹理未变化,却因噪声或外部条件变化,使窗口内像元整体变亮或变暗的情况,MRD 方法又容易产生虚警。

本文利用广义 Gamma 分布随不同的参数估计结果,可近似拟合多种分布的特点,来描述 SAR 图像杂波统计特性。采用信息论中用于计算拟合 PDF

与统计直方图间差异大小的 KL 散度概念,表征两幅 SAR 图像的变化程度,从而生成差异图。

如图 7,利用 MRD 方法对 2001 年与 2008 年的两幅天津市的 Radarsat 图像进行检测,所获取的差异图水域部分产生了大量虚警;利用基于广义 Gamma 分布的 KL 距离获取差异图,如图 8,可有效地避免这一问题。

为了进一步验证基于广义 Gamma 分布的 KL 差异图提取方法的优越性,本文从图 9 中选取了对应的 3 块样区, A 为西青区鸭淀水库、B 为津南水库、C 为北大港湿地。已知样区大小为 1186048 个像元,其中实际变化像元有 174608 个,未变化像元有 1011440 个。分别对该方法与 MRD 方法基于不同阈值时的检测率与虚警率进行统计,进而 ROC(receiver operating characteristics)曲线。

ROC 分析起源于统计决策理论,自 20 世纪 50 年代起应用于雷达信号观察能力的评价,最原始的用法是判断接受机从信号和噪音混合波形中提取有用信号的能力。自 2003 年起,Inglada 等将其拓展到 SAR 图像变化检测差异图提取方法的性能评价上,用于表现各算子检测率与虚警率间的相互关系。其主要用法是:视图像为一个变化与未变化的二分类总体,对所有可能的阈值,计算各算子检测率和虚



图 7 MRD 差异图



图 8 G-Gamma KL 差异图



图 9 原始图像样区选取

警率之间的组合，然后在坐标系中绘制并连接。当取值为阈值上限时，所有像元视作未变化，导致检

测率与虚警率都为 0，这与 ROC 曲线左下角的作业点是一致的；随着阈值的降低，检测率与虚警率相应增加；当取值为阈值下限时，所有像元视为变化，导致检测率与虚警率值都为 1，从而与 ROC 曲线右上角相一致。

根据霍春雷等(2008)可知，ROC 曲线下方覆盖面积越大，表示该方法检测效果越好，根据图 10，本文提出的广义 Gamma 交叉熵算子(红色)的检测效果要明显优于传统的 MRD(蓝色)差异图提取法，而基于瑞利的交叉熵算子(绿色)效果则位于两者之间。

3.3 差异图拟合分布函数选取

本文分别选用北京地区基于广义 Gamma 分布的 KL 差异图、天津地区基于广义 Gamma 分布的 KL 差异图，以及天津地区基于 Rayleigh 分布的 KL 差异图等 3 幅图像，通过调用 Kolmogorov-Smirnov (KS)与 Jensen-Shannon(KL)相结合的检验方法，对不同模型的 PDF 拟合情况进行了评估。

KS 检验是一种常用的无参估计，用来检验数据的分布是否符合一个理论的已知分布。自 1967 年提出以来，被众多学者广泛应用于各领域的统计模型拟合检验。由于 KS 检验需要使用分布模型的累积分布函数(CDF)，而广义 Gauss 模型 CDF 的两种求解方法：构造 PDF 的上界函数，以及随机微分方程，会因上界函数对应的随机数或反应扩散方程系数的选取情况，而对仿真结果产生影响。本文通过调用 2.2 节中提出的 KL 检验对广义 Gauss 模型，以及 KS 检验评估出的最佳拟合模型。进行评价比较，进而实现最优拟合模型的选取。

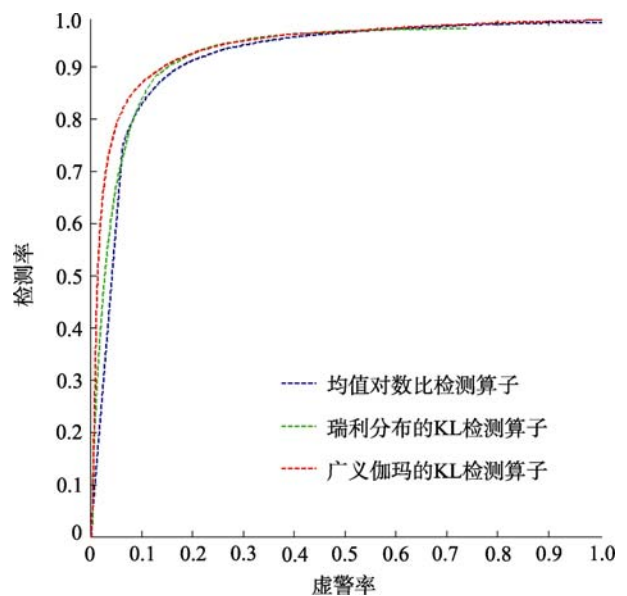


图 10 基于 MRD 与 G-Gamma 交叉熵的 ROC 曲线

从表 2 和表 3 可以看出, 对于北京地区基于广义 Gamma 分布的 KL 差异图, Rayleigh 与 Lognormal 联合分布函数的拟合情况最为理想; 而对于天津地区基于广义 Gamma 分布的 KL 差异图, G0 函数的拟合情况最为理想; 对于天津地区基于 Rayleigh 分布的 KL 差异图来说, Rayleigh 和 Lognormal 联合分布函数的拟合情况最为理想。可见, 广义 Gauss 方法虽然对 MRD 差异图拟合十分理想, 但对本文所提出的基于 KL 距离的差异图并不适用。由此证实, 若选取不同地物, 或不同分布模型进行 SAR 图像拟合, 所生成的 KLDIV 差异图可能会符合不同的分布。所以, 本文所使用方法是必要的, 也是可行的。

表 2 不同拟合分布模型的 KS 检验结果

| Kolmogorov – Smirnov 检验方法 | 北京市区 | 天津市 | 天津市 |
|---------------------------|-------------|-------------|-------------|
| | 广义伽玛 KL 差异图 | 广义伽玛 KL 差异图 | 瑞利分布 KL 差异图 |
| 对数正态 | 0.04593 | 0.059662 | 0.075721 |
| 伽玛 | 0.10155 | 0.030702 | 0.086152 |
| 瑞利 | 0.47975 | 0.10716 | 0.46306 |
| 韦布 | 0.08565 | 0.050324 | 0.08876 |
| K 分布 | 0.14910 | 0.041051 | 0.10292 |
| 联合分布 | 0.02193 | 0.027327 | 0.064636 |
| G0 分布 | 0.07289 | 0.026651 | 0.38563 |

表 3 8 种拟合分布模型的 KL 检验结果

| Jensen-Shannon 检验方法 | 北京市区 | 天津市 | 天津市 |
|---------------------|-------------|-------------|-------------|
| | 广义伽玛 KL 差异图 | 广义伽玛 KL 差异图 | 瑞利分布 KL 差异图 |
| G0 分布 | 0.0828 | 0.0473 | 0.1630 |
| 广义高斯 | 0.1900 | 0.2086 | 0.1704 |
| 联合分布 | 0.0473 | 0.0561 | 0.0271 |

3.4 阈值分割及结果评估

以天津市的两幅 Radarsat 图像为例(图 5), 首先提取基于广义 Gamma 模型的 KL 距离差异图(图 8), 调用 KS 检验(图 11)对各种分布模型的拟合情况进行评估。根据表 2 中第 2 列显示的评估结果, 可以看出, 适用于极不均匀区域的 G0 模型的拟合效果最好, 故使用基于 G0 模型的 KI 阈值分割方法(图 12)。

在 SAR 图像变化检测的研究领域中, 以 Lorenzo Bruzzone 为首的许多学者, 将研究重点放在了基于 MRD 差异图的广义高斯 KI 阈值分割方法的优化与拓展上, 取得了一定的进展。本文使用该方法对天津市 2001 年与 2008 年的两幅图像, 进行了变化检测处理。已知鸭淀水库于 2007 年 4 月完成的筑岛工程、津南水库于 2003 年开发了果木种植业与水产养殖业应用区, 而北大港湿地面积的近年来已大幅度缩减等。

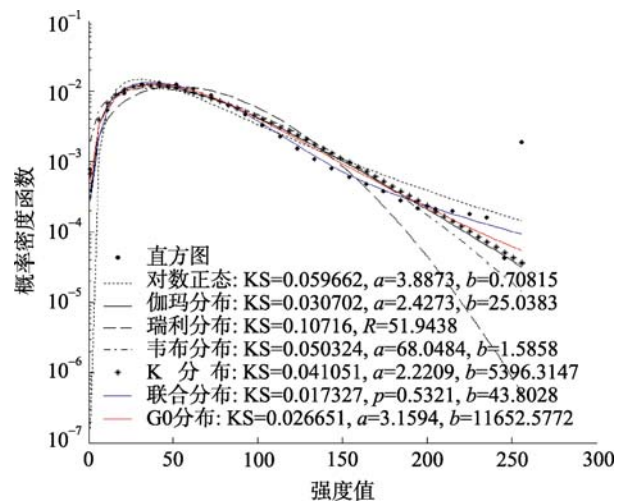


图 11 广义 Gamma KLDIV KS 检验



图 12 G-Gamma KLDIV 自动 KI 分割

为了直观地将本文的方法与该方法进行比较, 本文使用了数学形态学后处理及边界跟踪算法, 将得到的二值化掩模中变化区域的边界信息, 分别绘制于两幅原图像上(图 13、图 14)。

可以看出, 基于广义 Gauss 模型的 KI 阈值分割法较为有效地避免了部分 MRD 方法可能产生的, 水面波纹变化造成的虚警情况。但是, 无法从根本上解决位于大面积变化区域中的小面积不变区域无法检测的问题, 造成较多虚警。如实验结果所示, 本文所选用的方法, 有效地解决了这一问题, 成功的

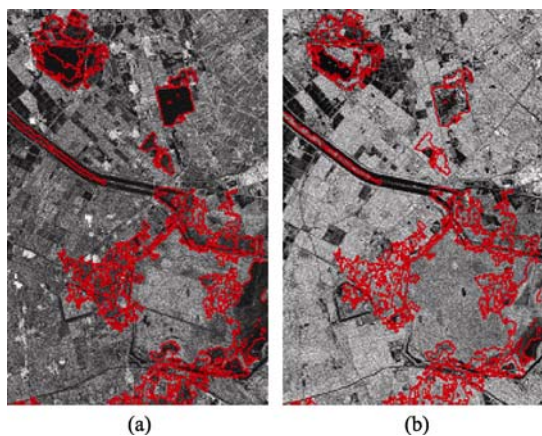


图 13 二时相基于 MRD 的 G-Gauss 分割
(a) 2001-11-14; (b) 2008-10-22

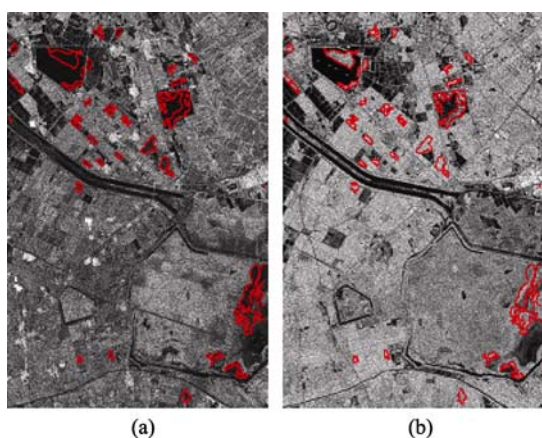


图 14 基于广义 Gamma 的 KL 差异图 G0 阈值分割
(a) 2001-11-14; (b) 2008-10-22

检测出基于广义 Gauss 模型的 KI 阈值分割方法中误判为变化的北大港小面积湿地, 以及津南水库中心未变化水域。简言之, 本文所使用的方法, 对于小面积变化区域的细节描述, 比基于 MRD 的广义 Gauss 阈值分割方法更为适用。

4 结论与展望

本文提出了一种基于广义 Gamma 分布的 KL 差异图提取及自适应 KI 阈值分割的新方法。该方法首次将广义 Gamma 模型运用到基于 KL 距离的差异图提取操作中, 有效地克服了传统 MRD 方法对局部纹理等特征信息的丢失问题; 同时, 将 KS 与 KL 检测相结合, 实现了自适应 KI 阈值分割。本文对天津市北辰区以南的 Radarsat-1 与 Radarsat-2 图像, 及北京市顺义区的两幅 Envisat-ASAR 图像进行了实验。经实验验证, 该方法能有效地通过对 SAR 图像统计特征的拟合, 较准确的获取了辐射值与纹理等特征信息, 使其效果比以往传统的变化检测方法, 要更

理想。尤其是对如农田种植物、湿地, 以及小面积建筑区域等类型的地物变化, 该方法的检测结果更为优越。关于算法效率的进一步优化, 以及与图像特征提取算法的进一步融合(Gamba, 2006)等, 将是下一步工作的研究重点。

REFERENCES

- Carvalho L M T and Fonseca L M G. 2001. Digital change detection with the aid of multiresolution wavelet analysis. *International Journal of Remote Sensing*, **4**(5): 3871—3876
- Chatelain F and Inglada J. 2008. Change detection in multisensor SAR images using bivariate gamma distributions. *IEEE Transactions on Image Processing*, **17**(3): 249—258
- Gamba P, Dell'Acqua F and Lisini G. 2006. Change detection of multi-temporal SAR data in urban areas combining feature-based and pixel-based techniques. *IEEE Transactions on Geoscience and Remote Sensing*, **144**(10): 2820—2827
- Gomes O, Combes C and Dussauchoy A. 2008. Parameter estimation of the generalized gamma distribution. *Mathematics and Computers in Simulation*, **79**(4): 955—963
- Huo Chun-lei. 2008. Object-level change detection based on multiscale fusion. *Acta Automatica Sinica*, **34**(3): 251—257
- Inglada J. 2003. Change detection on SAR images by using a parametric estimation of the Kullback-Leibler divergence. In Proc. IGARSS Toulouse, France
- Jiao Li-chen. 2008. Intelligent SAR Image Processing and Interpretation. Beijing: Science Press
- Kittler J and Illingworth J. 1986. Minimum error thresholding. *Pattern Recognition*, **19**(1): 41—47
- Kuang Gang-yao. 2007. Synthetic Aperture Radar Target Detection Theory Algorithm and Application. Beijing: University of Defense Technology Press
- Mercier G and Derrode S. 2004. SAR image change detection using distance between distributions of classes. *IEEE Transactions on Geoscience and Remote Sensing*, **74**(4): 3872—3875
- Mercier G and Inglada J. 2007. A new statistical similarity measure for change detection in multitemporal SAR images and its extension to multiscale change analysis. *IEEE Transactions on Geoscience and Remote Sensing*, **45**(5): 1432—1445
- Moser G. 2008. Conditional copulas for change detection in heterogeneous remote sensing images. *IEEE Transactions on Geoscience and Remote Sensing*, **46**(5): 1147—1153
- Moser G. 2007. Unsupervised change detection from multichannel SAR images. *IEEE Letters. Geoscience and Remote Sensing*, **4**(2): 278—282
- Moser G and Serpico S B. 2006. Generalized minimum-Error thresholding for unsupervised change detection from SAR amplitude imagery. *IEEE Transactions on Geoscience and Remote Sensing*, **44**(10): 2972—2982
- Oliver C. 2004. Understanding Synthetic Aperture Radar Images: SciTech Publishing
- Rignot E, Zyl J M and Van J. 1993. Change detection techniques for ERS-1 SAR data. *IEEE Transactions on Geoscience and Remote Sensing*, **31**(4): 896—906
- Sharifi K and Leon-Garcia A. 1995. Estimation of shape parameter for generalized Gaussian distributions in subband decomposition of video. *IEEE Trans. Circuits, Syst. Video Technol*, **1**(5): 52—56
- Uiaby F T and Kouyate F. 1986. Textural information in SAR images. *IEEE Transactions on Geoscience and Remote Sensing*, **24**(2): 235—245